ELECTRICAL RESISTIVITY FOR EVALUATION OF CONCRETE CORROSIVITY

F. Pruckner and O. E. Gjørv
Department of Building Materials
Norwegian University of Science and Technology, NTNU, Norway

Abstract

As soon as embedded steel in concrete structures becomes depassivated by carbonation or penetration of chlorides, the rate of steel corrosion is mainly controlled by oxygen availability and electrical resistivity. Above water, oxygen availability is normally not a limiting factor. Hence, the rate of steel corrosion will then be mostly controlled by the electrical resistivity. In the present paper, resistivity measurements are especially compared to relative humidity measurements at the same locations of a field structure and the influence of temperature is investigated.

1. Background

The electrical resistivity of concrete which is primarily controlled by permeability, degree of water saturation and the physico-chemical properties of the pore water solution, may for a portland cement concrete vary within a range of 1 to 1000 kΩcm [1]. For composite cements based on blast furnace slag, fly ash and silica fume, it may be even higher [2, 3]. The concrete resistivity may also depend on both salt contamination and temperature.

For a macrocell corrosion, the ohmic resistance is to a great extent determining the rate of corrosion, which can be described as [4]:

$$I_{corr} = \frac{\Delta U}{R_{an} + R_{cat} + R_{concrete}} \cdot \frac{1}{A_{an}}$$ eq. 1

with:

I_{corr} ....corrosion current ΔU .... driving force (potential difference)
R_{an} ....resistance at the anode R_{cat} .... resistance at the cathode
$R_{concrete}$ .....ohmic concrete resistance A_{an} .... area of the anode

In the case of ohmic control ($R_{concrete} > R_{an}$, R_{cat}), where the concrete resistivity is the governing factor for the corrosion process, eq. 1 can be simplified, and the corrosion current density becomes approximately inversely proportional to the resistivity:

$$i_{corr} \propto \frac{1}{\rho_{concrete}} \qquad\qquad eq. 2$$

Already in 1958, Gewertz et al. [5] observed that the rate of steel corrosion in concrete bridges almost became negligible for concrete resistivities above 50 to 70 kΩcm. Later on, low corrosion rates for a given concrete have mostly been associated with dry conditions, and much research has been focused on the effect of relative humidity.

According to González et al. [6], the corrosion activity is primarily controlled by the concrete resistivity when the saturation degree becomes less than 60%. For increasing concrete resistivity, the development of corrosion microcells is gradually hindered (Fig. 1).
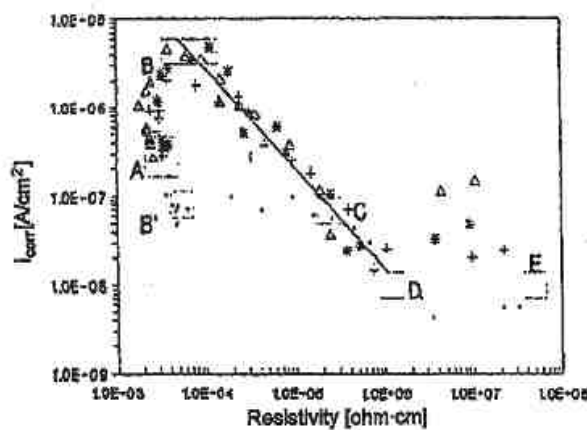

Fig. 1a: Relationship between electrical resistivity and the corrosion rate of embedded steel [6].
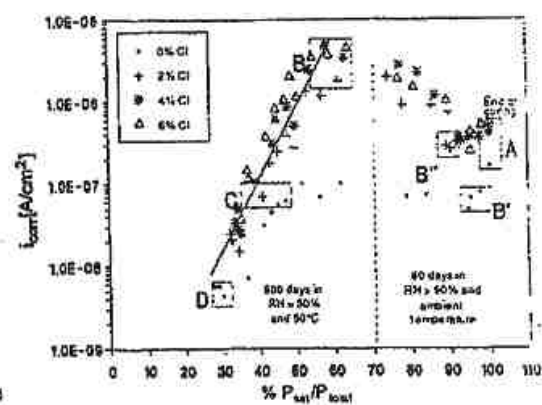
Fig. 1b: Influence of the degree of pore saturation on the corrosion rate of embedded steel [6].

For a pore saturation degree in the range of 60 % to 30 %, the corrosion rate is reduced logarithmic with the saturation degree for a chloride containing concrete, while for a non-chloride containing concrete, the corrosion rate remains more or less constant. Below a critical saturation degree of 30 %, the corrosion rate becomes negligible, and this level is therefore called a critical level of pore saturation (SD$_c$) [6]. At this level of saturation degree, all the capillary pores are dry. The relationship between moisture content and concrete resistivity can be described by the following empirical equation:

$$\rho = \frac{\rho_{SD=100\%}}{\left(\dfrac{SD}{100}\right)^n} \quad \text{or} \quad \log(\rho) = \log(\rho_{SD=100\%}) - n \cdot \log\left(\frac{SD}{100}\right) \qquad eq. 3$$

Analysis of the saturation degree-resistivity data from Sellevold [7] in the range of SD = 70 to 100 % fits this equation well as shown in Fig. 2:
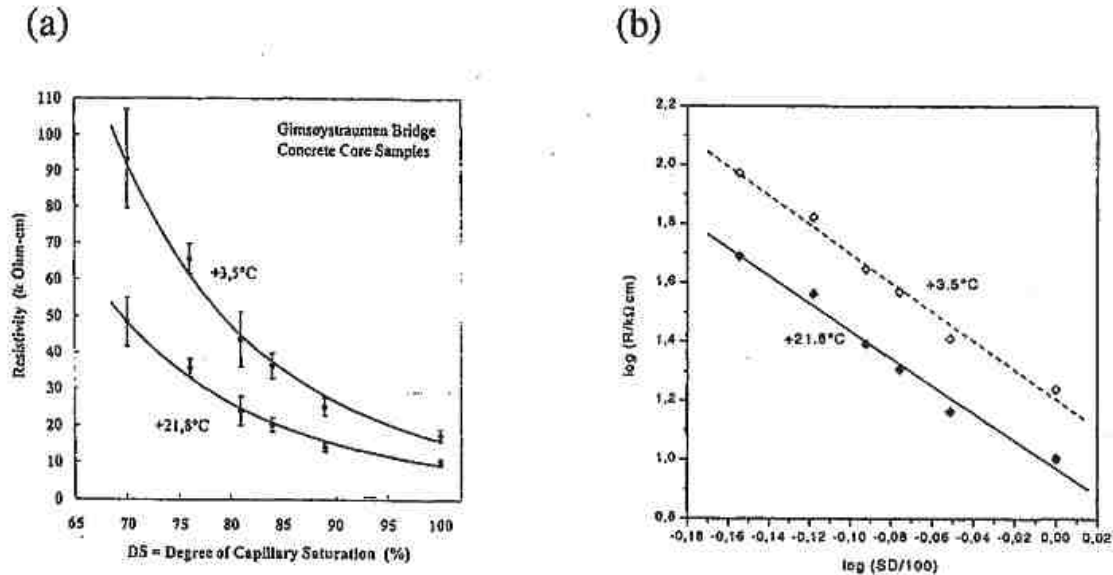
(a)
(b)

Fig. 2: (a): Relationship between saturation degree and concrete resistivity [7], (b): analysis of the same data using eq. 3.

By discussing the effect of temperature on the electrolytic resistivity, the effect of temperature on the properties of water should be considered first.

According to the ideal theory of electrolytic solutions which is valid both for ionic conductivity as well as for a diffusion process, the viscosity of water is the most important temperature dependent parameter affecting these properties. Since the ionic conductivity of an electrolyte is related to ionic mobility, similar temperature effects as for a diffusion process should be expected. In order to move a particle in a liquid, a minimum energy is needed. Since the probability for the energy of a molecule exceeding E_A is proportional to $e^{-E_A/RT}$, the mobility of the molecules in the liquid should follow this Boltzmann temperature dependence. Since the viscosity η is inversely proportional to the mobility of the particles, we should expect that

$$\eta = C \cdot \exp\left(\frac{E_A}{RT}\right)$$

eq. 4

implying that the viscosity should decrease exponentially with increasing temperature. This is also found to be the case, at least over a reasonably small temperature range. From the point of view of the ideal electrolytic theory, the effect of temperature on the electrolytic resistivity should follow the dependency of water viscosity. This is due to the following equations:

$$\Lambda = \sum_i |z_i| c_i u_i F \qquad \text{eq. 5}$$

$$u_i = \frac{|z_i| e_0}{6\pi \eta r_i} \qquad \text{eq. 6}$$

The relationship between the resistivity of an electrolyte and viscosity should therefore be:

$$\rho_\Omega = \frac{6\pi}{e_0 F \cdot \sum_i \dfrac{z_i^2 c_i}{r_i}} \cdot \eta \qquad \text{eq. 7}$$

Since the viscosity η is the only parameter depending on temperature, the constants can be drawn together leading to the following expression showing the temperature dependence of ρ_Ω:

$$\rho_\Omega = \rho_{\Omega,0} \cdot \exp\left(\frac{E_A}{RT}\right) \qquad \text{eq. 8}$$

which in short can be expressed as

$$\rho_\Omega = \rho_{\Omega,0} \cdot \exp\left(\frac{b(\rho_\Omega)}{T}\right) \qquad \text{eq. 9}$$

where $E_A/R = b(\rho_\Omega)$ and where $\rho_{\Omega,0}$ is the resistivity at the reference temperature (at $RT = E_A$). Since E_A for the viscous flow of water is 17 kJ/mol, the constant $b(\rho_\Omega)$ should ideally be 2072 K. However, for concrete it has been found that $b(\rho_\Omega)$ is dependent on the saturation degree, varying from 4500 K at 20 % saturation to 2500 K at 80% saturation and 2000 K at 100% water saturation. Additionally it has been found, that the constant $b(\rho_\Omega)$ of the pore solution is approximately 1750 K [8].

2. Experimental

In representative locations of two concrete decks of a garage building, measurements of both electrical resistance (ρ), relative humidity (RH) and temperature (T) were carried out. On top of all the decks, the concrete was protected by an approximately 5 mm thick polyurethane coating, while underneath, the concrete was protected by an acrylic CO_2 stopping membrane.

In each concrete deck, holes were drilled in the representative locations. For the electrical resistance, the measurements were carried out between pairs of stainless steel bolts that was embedded in the holes by use of mortar. The distance between the bolts

was 30 mm, and the bolts were exposed at depths varying from 10 to 50 mm from the concrete surface.

The electrical resistance was recorded using AC-current at 1 kHz, and the resistivity calculated by use of the following equation [9]:

$$\rho = \frac{h}{\ln\left(\dfrac{a - \dfrac{d}{2}}{\dfrac{d}{2}}\right)} \cdot \frac{U}{I} \qquad \text{Eq. 10}$$

ρ .... resistivity
U/I (=R) .... measured resistance
h .... length of the electrodes
d .... diameter of the electrodes
a .... distance between the electrodes

For the measurements of relative humidity (RH) and temperature [T], the holes were 50 mm deep and had a volume of approximately 3 cm³. The measurements were carried out by use of a commercial hygrometric sensor of type Hygrotem III, which continuously records the two variables RH and T. The sensing element of the humidity probe was made of a hygroscopic material, in which the dielectric properties are changing with the ambient RH. The interval between two consecutive measurements was one hour. Hence, a monitoring period of one year delivers more than 8000 data points.

3. Results and Discussion

In Fig. 3 the typical development of electrolytic resistivity, relative humidity and temperature in two different concrete decks is presented. In the one case, the sensors were installed into the ceiling of the top-deck of the garage building directly exposed to sunshine, rain and snow (Case A), while in the other case, the sensors where installed into the ceiling of the ground floor of the garage, where the diurnal temperature effects are less pronounced (Case B). In Case A, the concrete was also contaminated with chlorides, while in Case B there was no chlorides. Fig. 3 shows the measurements of ρ, RH and T, for the two cases over a period of eight months.

The measured concrete resistivities at ambient temperature have been transformed into resistivities for a standard temperature of 25 °C using eq. 11:

$$\rho_\Omega(298\,\text{K}) = \rho_\Omega(\text{T}) \cdot \exp\left[\frac{E_A}{R}\left(\frac{1}{298\,\text{K}} - \frac{1}{T}\right)\right] \qquad \text{eq. 11}$$
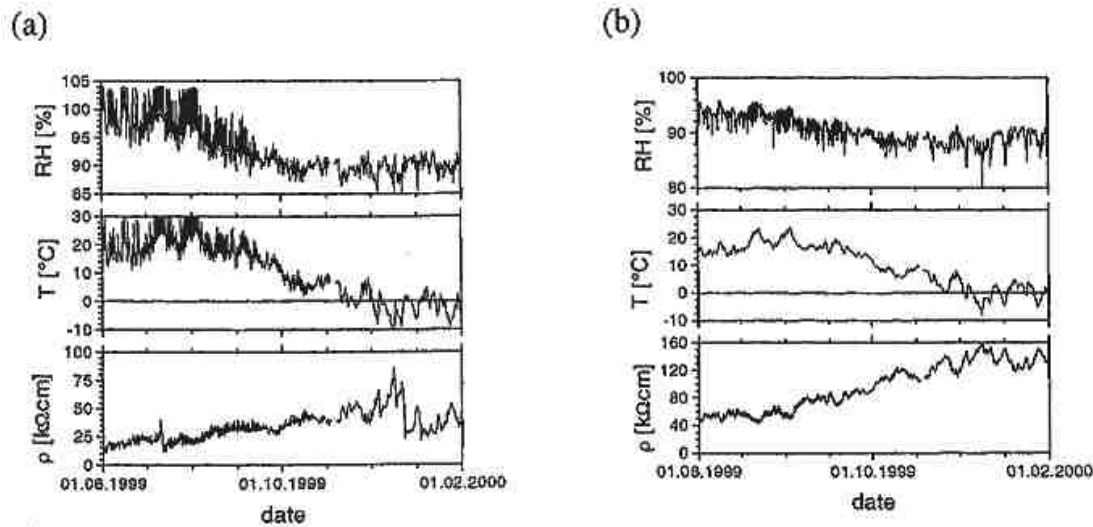
which has been derived from eq. 8.

Fig. 3: Relative humidity, temperature and concrete resistivity in two locations of a garage deck. (a): ceiling - top floor - Case A; (b): ceiling - ground floor - Case B.

The development of temperature compensated resistivities are shown in Fig. 4. After the compensation for temperature, the change of resistivity should only be due to possible changes of moisture content in the concrete and/or changes in the electrolytic composition of the porewater. As shown in Fig. 4, the variations of compensated resistivity values are small compared to the variations of temperature. Therefore, the temperature is obviously the parameter of strongest influence. The value for the activation energy E_A was 30 kJ/mol for both cases.

In Case A of Fig. 4, a sudden decrease of around 50% of the resistivity can be observed, and in Fig. 5, the period where this decrease happened is shown at a larger scale. As can be seen, the step-decrease took place at a time when the temperature exceeded 0 °C (Fig. 5). Therefore, this effect is probably related to the change in the viscosity of water at the freezing point.
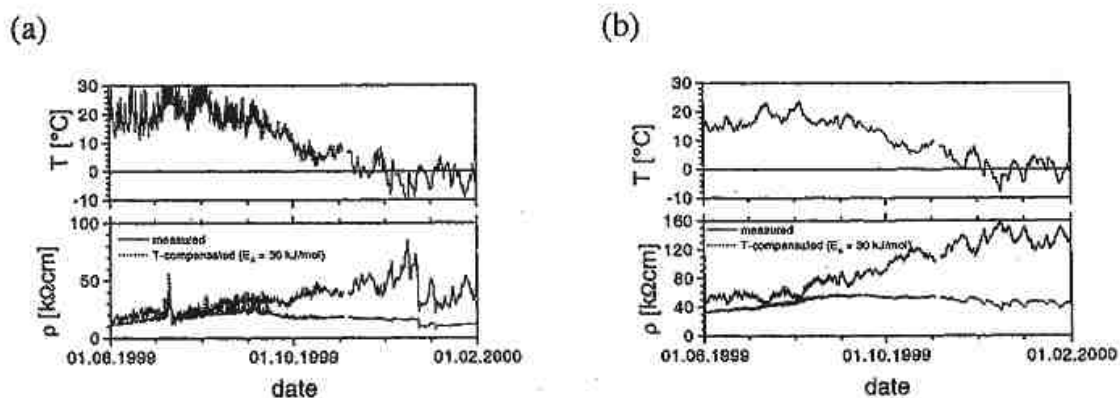

Fig. 4: Development of the temperature compensated resistivity values with time for Case A (a) and Case B (b).
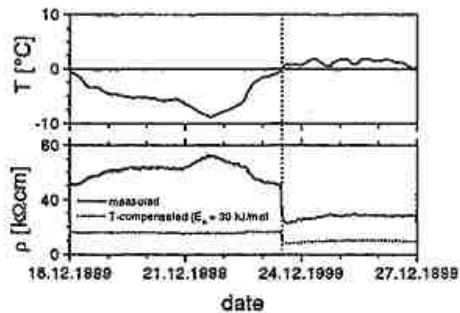
Fig. 5: Sudden decrease of the concrete resistivity (Case A) when the temperature in the concrete exceeds 0 °C.

After the effect of temperature on the concrete resistivity is eliminated, the resistivities can be compared with the changes in the relative humidity of the concrete. Also the humidity values have to be temperature compensated as discussed in ref. [10]. After this compensation, an averaging procedure for the RH values in was performed order to reduce the amount of scatter.

The smoothening of the active data was performed by averaging the adjacent data points. The smoothened value of index i is the average of the data points in the interval [i-n, i+n]. n = 100 was chosen for the treated cases in this work. Since, the measurement interval was 60 min. the smoothened value is the result of the averaging of observations from approximately one week. The resulting plots are shown in Fig. 6.

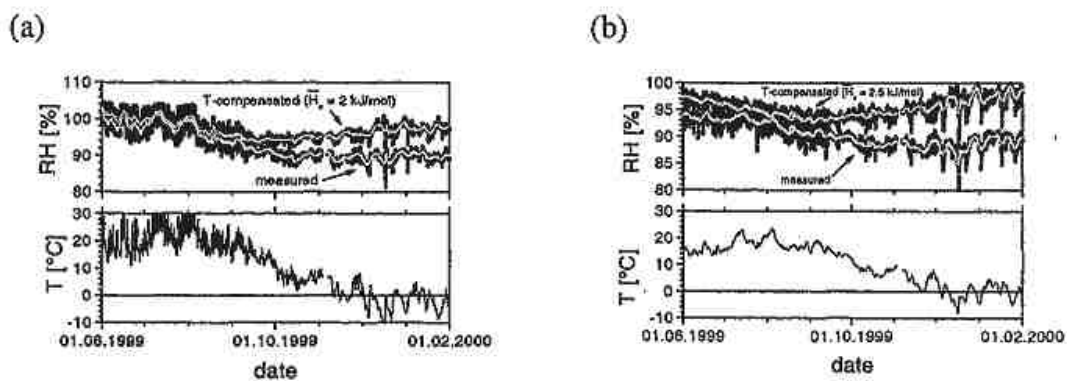(a)   (b)

Fig. 6: Temperature compensated and smoothened curves for the relative humidity measurements in concrete (a): Case A, (b): Case B.

In Fig. 7 the concrete resistivities are compared with the relative humidities in the concrete. In Fig. 7a the observed values of RH(T) vs. ρ(T) without temperature compensation are plotted against each other, where the humidity values have been smoothened using the procedure of adjacent averaging (n = 100). In Fig. 7b the temperature compensated and smoothened RH values have been plotted against standard resistivity values ($RH_{298 K}$ versus $\rho_{298 K}$).
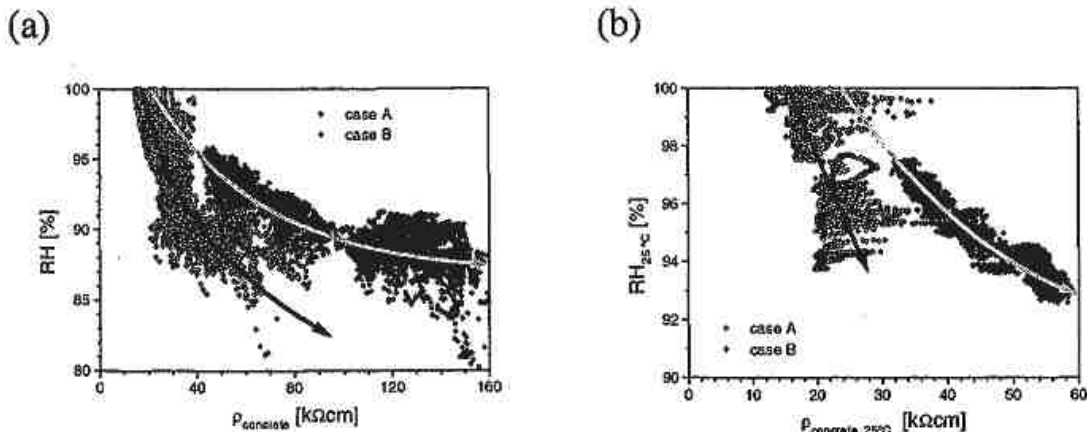
2076

Fig. 7: Correlation between RH- and ρ-measurements in concrete (a): uncompensated values and (b): temperature compensated values.

In Fig. 7, the advantage of using electrical resistivity measurements compared to relative humidity measurements as a basis for assessment of concrete corrosivity is clearly demonstrated. The two cases discussed represent concretes of similar quality, where one was salt contaminated due to embedded chlorides (Case A), while in Case B no chlorides were present. For Case A, a change in the relative humidity of the concrete does influence the resistivity of the concrete far less than that for Case B. For Case A, a decrease of RH from 100 to 85 % only gives an increased ρ by a factor of around 3, while for Case B, the factor is around 8, taking the non-temperature compensated values into the calculations. For the salt contaminated concrete, a certain drying out of the concrete pores causes an increased ionic concentration of the remaining pore water solution, which is counteracting an increased resistivity. Since the corrosion rate in salt contaminated concrete is very much controlled by the electrolytic concrete resistivity, RH-measurements only give limited information for a judgment of the concrete corrosivity.

3. Conclusions

As discussed in the present paper, the resistivity is very much controlled by concrete porosity, relative humidity, temperature and salt contamination. Since an increased degree of saturation decreases the ionic concentration of the porewater, the observed difference in concrete resistivity of salt contaminated concrete in dry and wet condition was far lower than that for concrete without any salt contamination. This means for the case of resistance controlled corrosion processes that monitoring of concrete resistivity should be a better tool for evaluation of concrete corrosivity than monitoring of relative humidity.

4. Acknowledgement

5. References

1. Gjørv, O.E., Vennesland, Ø., and El-Busaidy, A.H.S., 'Electrical Resistivity of Concrete in the Oceans', Paper OTC 2803, Offshore Technology Conference, Houston (1977) 581-588.
2. Vennesland Ø. and Gjørv, O.E., 'Silica Concrete - Protection Against Corrosion of Embedded Steel', Proceedings, Fly Ash, Silica Fume, Slag and other Mineral By-Products in Concrete, ACI SP 79-38, Ed. by M. Malhotra (1979) 719-729.
3. Fiore, S., Polder, R.B. and Cigna, R., 'Evaluation of the Concrete Corrosivity by Means of Resistivity Measurements', Proceedings, Corrosion of Reinforcement in Concrete Construction, Ed. by C.L. Page, P.B. Bamforth and J.W. Figg, SCI (1996) 273-282
4. F. Hunkeler, F., 'Monitoring of Repaired Reinforced Concrete Structures by Means of Resistivity Measurements', Materials Science Forum, 247 (1997) 93-106.
5. Gewertz, M.W., Tremper, B., Beaton, J.L. and Stratfull, R.F., 'Causes and Repair of Deterioration to a Californian Bridge due to Corrosion of Reinforcing Steel in a Marine Environment', Highway Research Board Bulletin, 182 (1958) 41.
6. González, J.A., López, W., and Rodríguez, P., 'Effects of Moisture Availability on Corrosion Kinetics of Steel Embedded in Concrete', Corrosion, Vol. 49 (1993) 1004-1010.
7. Sellevold, E.J., 'Resistivity and Humidity Measurements of Repaired and Non-Repaired Areas in Gimsøystraumen Bridge', Proceedings, 'Repair of Concrete Structures, From Theory to Practice in a Marine Environment', Ed. by A. Blankvoll, Norwegian Public Roads Administration, Oslo (1997), pp. 283-295.
8. Raupach, M., 'Effect of Temperature on Chloride Induced Steel Corrosion in Concrete', Proceedings, EUROCORR'97, Ed. by E. Bardal, Trondheim (1997), 431-438.
9. Carassiti, F., Proverbio, E. and Valente T., 'Corrosion State Evaluation of Steel in concrete by Resisitivity and Polarization Resistance Measurement', Materials Science Forum, (1992) 647-658.
10. Pruckner, F and Gjørv, O.E., 'Relative Humidity Measurements in Concrete', paper submitted to the Third International Conference on Concrete under Severe Conditions, CONSEC'01.